

# The Chaotic Nature of TRAPPIST-1 Planetary Spin States

Alec M. Vinson,<sup>1\*</sup> Daniel Tamayo<sup>2</sup>, & Brad M. S. Hansen<sup>1</sup>

<sup>1</sup>Mani L. Bhaumik Institute for Theoretical Physics, Department of Physics and Astronomy, University of California, Los Angeles, CA, 90095, USA

<sup>2</sup>Department of Astrophysical Sciences, Princeton University, Princeton, NJ, 08544, USA

Accepted XXX. Received YYY; in original form ZZZ

## ABSTRACT

The TRAPPIST-1 system has 7 known terrestrial planets arranged compactly in a mean-motion resonant chain around an ultra-cool central star, some within the estimated habitable zone. Given their short orbital periods of just a few days, it is often presumed that the planets are likely tidally locked such that the spin rate is equal to that of the orbital mean motion. However, the compact, and resonant, nature of the system implies that there can be significant variations in the mean motion of these planets due to their mutual interactions. Such fluctuations create a moving target between the spin rotation rate and the orbital mean motion, which we show can then have significant effects on the spin states of these planets. In this paper, we analyze, using detailed numerical simulations, the mean motion histories of the three planets that are thought to lie within or close to the habitable zone of the system: planets d, e, and f. We demonstrate that, depending on the strength of the mutual interactions within the system, these planets can be pushed into spin states which are effectively non-synchronous. We find that it can produce significant wobble of the spin state, if not complete circulation in the co-rotating frame. We also show that these spin states are likely to be unable to sustain long-term stability, with many of our simulations suggesting that the spin evolves, under the influence of tidal synchronization forces, into quasi-stable attractor states, which last on timescales of thousands of years.

**Key words:** planets and satellites: dynamical evolution and stability – stars: low-mass

## 1 INTRODUCTION

The search for habitable planets around nearby stars has spurred a great interest in the lowest mass stellar hosts, because terrestrial planets are physically larger and more massive relative to the host, and therefore easier to detect and characterize. Furthermore, the habitable zone is estimated to lie closer to the fainter low mass stars, making the chance of a transit detection greater. For such reasons, the TRAPPIST-1 exoplanetary systems has sparked much interest in the scientific community, with seven planets observed in a compact configuration orbiting close to an ultra-cool dwarf star. Several of the reported planets may lie in a mean motion resonant chain, and several lie near or within the estimated habitable zone. With orbital periods on the order of just a few days, tidal interactions between the planets and the host star are expected to be significantly stronger than those the Earth experiences from the Sun. This would suggest that these planets, or any planets orbiting within the habitable zone around such small and cool stars, would almost certainly be tidally locked into a synchronous spin state, wherein the planet’s spin period and orbital period are equal to each other. This is often considered as a significant barrier to the habitability of such planets, because of the extreme temperature differences such conditions engender across the face of the planet.

In previous work (Vinson & Hansen 2017), we proposed a

potential solution to this tidal locking problem. For a synchronously rotating body (like the Earth’s moon), its spin rate equals its orbital rate so as to always present the same face toward the primary. However, planets in, or near, a mean motion resonance undergo mean motion variations. These variations create a moving target for the synchronicity of the spin rate to the mean motion, which can affect the spin in such a way that it stably librates in the co-rotating frame about an equilibrium point, or else circulates completely, resulting in full, stable, stellar days. We found that timescales of libration or circulation were such ( $\lesssim 1$  years for a TRAPPIST-1 inspired system) that they were less than the atmospheric response time of  $\lesssim 10$  years for Earth-like planets (Spiegel et al. 2008). Thus, this model provides a potential mechanism to prevent the predicted atmospheric collapse caused by the freezing of volatiles on the night side for planets with atmospheres below certain threshold densities (Kasting et al. 1993; Joshi et al. 1997; Wordsworth 2015).

In our previous paper, we addressed only how the spin of the a planet would be affected by a single companion of much greater mass near resonance. In reality, planets in multi-planet systems tend to have similar masses (Millholland et al. 2017; Weiss et al. 2018), and thus mutually interact. Additionally, many planetary systems are highly multiple and can even form multi-resonant chains, with TRAPPIST-1 as the prime example. In this paper, we therefore incorporate the effects of multiple planets in as resonant chain on a planet’s spin state, using the TRAPPIST-1 system to showcase our model and possible behaviors.

\* E-mail: vinson@astro.ucla.edu

We use N-body integrations from [Tamayo et al. \(2017\)](#) to provide the orbital evolution of TRAPPIST-1-like systems. From these we extract time series of the planets’ mean motion variations as input for the spin model from our original paper, which we reintroduce in §2. Taking N-body integrations for a range of resonant initial conditions near the observed planetary configuration, we obtain a variety of possible orbital behaviors, and investigate how they affect the spin states given our spin model.

In §2 we reintroduce our spin model and describe how we incorporate orbital integrations into it. In §3 we present our findings, and in §4 discuss the significance and some implications of our results. §5 summarizes our findings and provides some concluding remarks.

## 2 MODEL AND METHODS

We describe the planetary spins using the same basic framework presented in [Vinson & Hansen \(2017\)](#). Thus we will consider a system with a planet of mass  $m$  orbiting a star of mass  $M_*$  with zero obliquity. We let  $A$ ,  $B$ , and  $C$  be the principal moments of inertia of the planet with  $C$  being the moment about the spin axis and  $A$  being the moment about the long axis of the planet in the plane of the orbit such that  $B > A$ . We define  $\theta$  to be the angle formed between the long axis of the planet and a stationary line in the inertial frame, and another angle  $\gamma \equiv \theta - M$ , where  $M$  is the mean anomaly.  $\gamma$  then roughly corresponds to the longitude of the substellar point for a planet on a near-circular orbit. We then apply the equation of motion for  $\gamma$  as derived and presented in [Goldreich & Peale \(1966, 1968\)](#) and [Murray & Dermott \(1999\)](#), under the assumption that  $\dot{\theta} \approx n$

$$\ddot{\gamma} + \text{sign}[H(e)] \frac{1}{2} \omega_S^2 \sin 2\gamma + \dot{n} = 0 \quad (1)$$

Where  $n = \dot{M}$  is the mean motion,  $H(e)$  is a power series in orbital eccentricity  $e$ , and  $\omega_S^2 = 3n^2 \left( \frac{B-A}{C} \right) |H(e)|$ .

However, a crucial difference between equation 1 presented here and that presented in other sources is that we do not dispose of the  $\dot{n}$  term on the presumption that it should be insignificant. In this case, one is left with the differential equation for a pendulum in the variable  $\gamma$ . In fact, as shown in our previous work, the  $\dot{n}$  term can provide a substantial driving that alters the evolution of  $\gamma$  if there is a companion near a mean-motion resonance which can induce strong mean motion oscillations.

Previously ([Vinson & Hansen 2017](#)), we applied the “pendulum model” presented in [Murray & Dermott \(1999\)](#) to describe the  $\dot{n}$  term in equation 1, wherein  $n$  evolved as a simple pendulum under the effects of a single companion planet in resonance. Thus, equation 1 described something analogous to a forced pendulum for the evolution of  $\gamma$ , with the simple case having two stable equilibria corresponding to opposite faces of the planet along the planet’s long axis pointing to the host star. The main difference from a typical forced pendulum is that our forcing term itself behaved like a pendulum instead of the more typical case of a simple sinusoid. The forced pendulum is a popular topic in dynamical studies due to its interesting chaotic behaviors when the natural and driving frequencies are close in value. Indeed, after incorporating tidal damping effects in the model, our results in [Vinson & Hansen \(2017\)](#) depicted a wide range of interesting limit cycles for example systems based off of the TRAPPIST-1 and K00255 planets.

However, many systems are found to be highly multiple, including the TRAPPIST-1 system that inspired much of our work. To

have a fuller understanding of the possible behaviors of the spin, we must then expand the model to incorporate the effects of multiple resonant companions. This is the main difference between the work presented in this paper and our previous one: we now consider the effects of *multiple*, mutually interacting companions in or near mean motion resonances in order to understand how our model applies to resonant-chain systems such as TRAPPIST-1, wherein there are seven planets compactly arranged into a long resonant chain. This introduces a more difficult problem in describing how exactly the mean motion of any particular planet varies in time, with interactions from many companions. We therefore use N-body integrations of the TRAPPIST-1 system by [Tamayo et al. \(2017\)](#) to calculate the variations in the orbital eccentricities and mean motions numerically.

TRAPPIST-1 presents a very attractive system as a compact analog of the inner Solar System, with the seven planets contained within the system receiving between about 10% to 400% the stellar irradiation of the Earth. As first announced by [Gillon et al. \(2017\)](#), the inner six planets in the system form the longest known near-resonant chain of exoplanets, with orbital period ratios of approximately 8/5, 5/3, 3/2, 3/2, and 4/3 between planets c, d, e, f, and g, respectively, and their nearest inner companion. We also note that the period ratios of e to d, f to e, and g to f, suggest that the resonances are of first-order, which also suggest larger variations in  $\dot{n}$  as can be seen in the model described in [Vinson & Hansen \(2017\)](#).

### 2.1 Tidal Damping

Tidal effects on stellar and planetary orbits is a long-studied subject (see [Ogilvie \(2014\)](#) for a review). Tidal forces between planets and their host star are expected to be exceptionally strong in systems such as TRAPPIST-1 due to the close proximity between the planets and the host star. In the simple unforced case, this damping would push planets into synchronous spin-orbit states. We use the same formalism to describe tidal dissipation in this work as we did previously in [Vinson & Hansen \(2017\)](#), which we briefly describe in this section.

Based on the work of [Hut \(1981\)](#) and [Eggleton et al. \(1998\)](#) on tidal dissipation, we use equations (4) and (14) of [Hansen \(2010\)](#) to describe tidal dissipation on  $\gamma$  with

$$\ddot{\gamma} = -\frac{15}{2} \dot{\gamma} \frac{M_*}{m} \left( \frac{R}{a} \right)^6 M_* R^2 \sigma \quad (2)$$

where  $R$  is the planetary radius and  $a$  is the semi-major axis of the orbit. The strength of the dissipation is described in terms of a bulk dissipation constant  $\sigma$ , which can then be calibrated to desired values of the tidal parameter  $Q$ .

There is growing literature on the mechanisms of tidal dissipation in Earth-like planets ([Efroimsky & Lainey 2007](#); [Makarov & Efroimsky 2013](#); [Ferraz-Mello 2013](#); [Correia et al. 2014](#)), but we will use the simpler formalism of equation 2, which is sufficient for illustrative purposes and has the attractive quality that it avoids unphysical discontinuities by having tidal torque going to zero as  $\dot{\gamma}$  goes to zero. In particular, we wish to focus on the spin behavior driven by changes in the forcing without contamination by spin flips associated with abrupt changes in the sign of the spin damping forces.

Adding equation 2 to equation 1, we get our full equation of motion

$$\ddot{\gamma} + \frac{1}{2} \omega_S^2 \sin 2\gamma + \dot{n} - \epsilon \dot{\gamma} = 0 \quad (3)$$

where we let  $\epsilon = \frac{15}{2} \frac{M_*}{m} \left(\frac{R}{a}\right)^6 M_* R^2 \sigma$  define the strength of the dissipation. We note that while the spin evolution depends on the orbital behavior through  $\dot{n}$  and the eccentricity dependence in  $\omega_S$ , the spin has such negligible angular momentum compared to the orbit that the spin does not feed back on the orbital evolution. This allows us to simply plug in the orbital histories from N-body integrations to calculate the spin evolution.

## 2.2 Setup

To extract orbital parameters, we use the numerical integrations of Tamayo et al. (2017), which simulated a range of initial conditions near the observed resonant configurations of TRAPPIST-1. These spanned configurations at or near the centers of the observed resonant chain where eccentricities and mean motions remain nearly constant (i.e., low spin forcing), to ones near their separatrices where the orbits undergo larger, chaotic oscillations (i.e., strong spin forcing). These integrations thus can span range of dynamical behaviors, but we note that other works have determined better fits to the actual TRAPPIST-1 system (e.g. Gillon et al. 2017; Grimm et al. 2018). However, we wish to illustrate behaviors for a wide range of possibilities that can be applied not only to TRAPPIST-1, but to similar systems as well.

The integrations in Tamayo et al. (2017) were performed using the WHFAST integrator (Rein & Tamayo 2015) in the REBOUND N-body package (Rein & Liu 2012), with a timestep of 7% of the innermost planet’s orbital period. Details of their initialization by migrating them into the observed resonant chain with parametrized disk forces can be found in Tamayo et al. (2017). We extracted their publicly available<sup>1</sup> SimulationArchives, which allow for fast, parallel extraction of system parameters at arbitrary times (Rein & Tamayo 2017), and sampled eccentricities and mean motions at a cadence of 10% of the orbital period for each planet. With the mean-motion and eccentricity histories, we then used spline interpolation so that we could extract values of mean motion  $n$ ,  $\dot{n}$ , and eccentricity  $e$ , at arbitrary times to feed into equation 3 and perform an adaptive time-step, Fourth-Order Runge-Kutta integration to find the evolution of the spin parameter  $\gamma$ .

Choices also need to be made in regards to our tidal damping strengths, which can result in different behaviors. We choose to calibrate equation 2 to two different damping strengths. Studies suggest a tidal parameter  $Q \sim 10$  for the Earth, exerted primarily by pelagic turbulence in the oceans (Egbert & Ray 2000), so we will take this as our stronger damping estimate. For a water-poor terrestrial planet, we adopt  $Q = 100$  as our weaker damping, based on estimates for Mars (Lainey et al. 2007).

Finally, we focus on the spins of planets d, e, and f (while under the influence of all other companions in the system). Much of our interest in this problem is motivated by habitability questions, and these three planets all lie within the estimated habitable zone (Kopparapu et al. 2013, 2016). These planets, while likely to have experienced water loss during the host star’s  $\sim 1$  Gyr long pre-main sequence phase, are also likely to still have been able to retain significant oceans depending on initial water levels (Bolmont et al. 2017).

<sup>1</sup> <https://github.com/dtamayo/trappist>

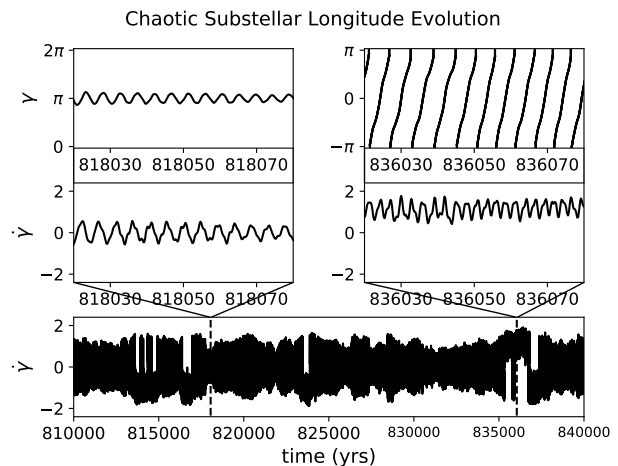


**Figure 1.** Example simulation of spin of planet 1f with  $\gamma$  plotted against time, wherein we set  $Q = 100$ . Years are used for units involving time. The bottom panel depicts the long-term evolution of  $\dot{\gamma}$  over several hundred thousands of years. The top four panels zoom in to depict two different types of behavior that occurs in this particular simulation, with the middle panels depicting evolution of  $\dot{\gamma}$  and the top panels depicting evolution of  $\gamma$ . On the left panels we observe libration of  $\gamma$  about  $\pi$ . On the right panels we observe a time when there is full circulation of  $\gamma$ , which can remain quasi-stable for approximately  $10^3$  years. Overall, this simulation depicts a chaotic evolution of the spin state, switching among librating and circulating states.

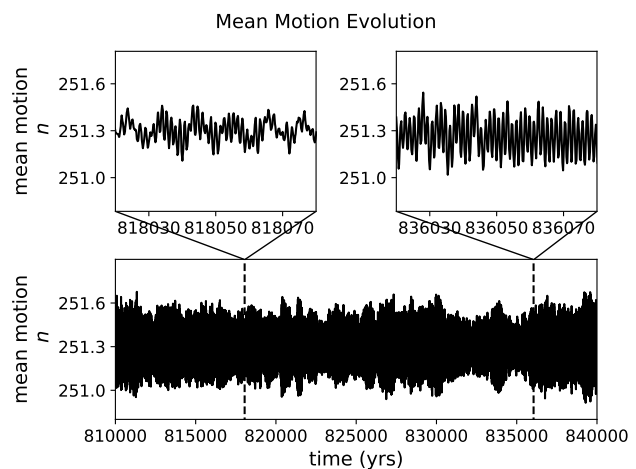


**Figure 2.** Example simulation of planet 1f depicting evolution of mean-motion  $n$  versus time taken from a Rebound simulation. This is used as input for our spin model, a corresponding simulation of which is shown in Figure 1. The bottom panel presents long-term evolution of  $n$ , while the top two panels zoom in to depict behavior at different instances in time. We can compare this to Figure 1 to see how the mean-motion input affects the spin state. We find that the most dominant frequency when performing a Fourier Transform on  $n$  is  $\omega_M = 5.076 \text{ yr}^{-1}$ . We also find that the standard deviation of  $\dot{n}$ , which we can use as a proxy for overall forcing strength, is  $\sigma(\dot{n}) = 0.548 \text{ yr}^{-2}$ . We note, however, that  $\sigma(\dot{n})$  varies throughout the simulation, and we can observe here that the mean-motion has larger variations in the top right panel than in the top left panel, corresponding to circulating and librating states for the spin argument  $\gamma$  as seen in Figure 1, which is suggestive that the behavior of the spin depends strongly on the strength of mean-motion variations.

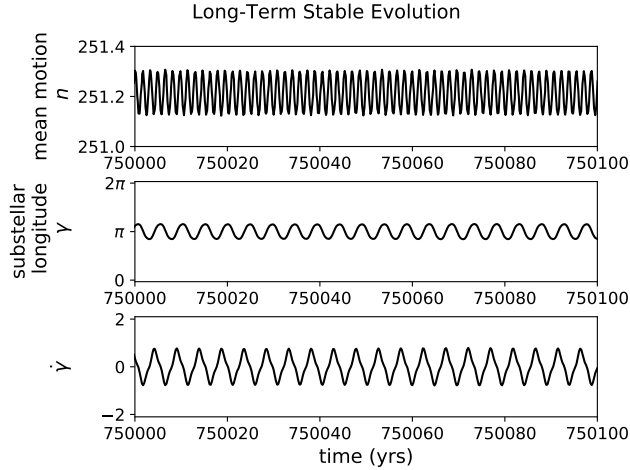


**Figure 3.** Example simulation of planet 1f depicting evolution of mean-motion  $n$  in the top panel,  $\gamma$  in middle panel, and  $\dot{\gamma}$  in the bottom panel. This is an example of a simulation which has a very stable evolution in mean-motion which is strongly dominated by just one frequency,  $\omega_M = 4.18 \text{ yr}^{-1}$ , as shown in the Fourier transform in Figure 5. Thus, we also observe a stable evolution of the spin argument  $\gamma$ , wherein we observe a stable libration of  $\gamma$  about  $\pi$ . We also note that the standard deviation of  $\dot{n}$ , which we use as a proxy for forcing strength, is  $\sigma(\dot{n}) = 0.263 \text{ yr}^{-2}$ .

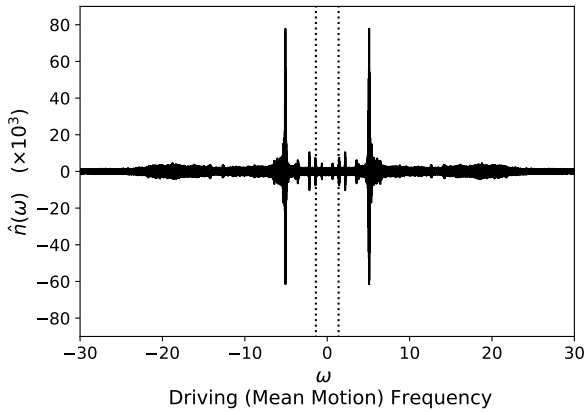


**Figure 4.** Here we see the frequency spectrum of the mean motion  $n(t)$ , denoted  $\hat{n}$ , for the entire time range of the simulation corresponding to Figure 2. Here we see that, while there is a primary frequency which dominates in the behavior of  $n(t)$ ,  $\omega_M = 5.076 \text{ yr}^{-1}$ , there are also some secondary frequencies which can change the behavior of  $n$ , and thus its influences on the spin argument  $\gamma$ . We also plot vertical dashed lines to indicate the spin frequency for natural libration for planet f,  $\omega_S = 1.38 \text{ yr}^{-1}$ .

### 3 RESULTS

We can largely describe the REBOUND simulations, in relevance to our spin model, in terms of the strength of mean-motion variations, as well as the frequencies of the mean motion variations. We use various outcomes from different initial conditions of REBOUND simulations of the orbital parameters of the TRAPPIST-1 system, picked to span a range in forcing strength from negligible to strong

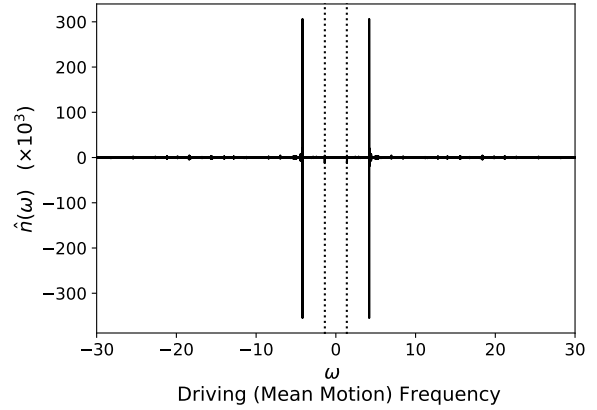


**Figure 5.** Here we see the frequency spectrum of the mean motion  $n(t)$ , denoted  $\hat{n}$ , for the entire time range of the simulation corresponding to Figure 3. Here we see that the evolution of  $n$  can largely be described in terms of just one dominant frequency,  $\omega_M = 4.18 \text{ yr}^{-1}$ , which is approximately three times the natural spin frequency  $\omega_S$ . We also plot vertical dashed lines to indicate the spin frequency for natural libration for planet f,  $\omega_S = 1.38 \text{ yr}^{-1}$ .

<sup>2</sup> (see horizontal axis of Figures 6-11), and use these as inputs for our own spin model detailed in this paper. Many of the simulations are dominated by a primary frequency of the mean-motion variations, with many others manifesting strong secondary frequencies. We use eighteen different simulations as input for our spin model, ranging from very low amplitude librations of the mean motion to higher amplitude variations, all of which are long-term stable configurations (Tamayo et al. 2017).

In this paper we look at those planets closest to the proverbial habitable zone: planets d, e, and f. With 18 different REBOUND simulations to apply to each of these planets, coupled with two different tidal strengths we choose to test ( $Q = 10$  and  $Q = 100$ ), we have a total of 36 different simulations of the spins of each of these three planets. We observe a variety of different behaviors that emerge from different integrations. These include integrations wherein the spin of the planet remains effectively purely synchronous, with very small librating amplitudes. Other simulations depict higher amplitude librations in the spin, while others even showcase periods of complete circulation. However, most of the realizations we studied exhibit chaotic evolution, with the spin often alternating between

<sup>2</sup> REBOUND simulations used by file name found at <https://zenodo.org/record/496153>:

IC111K1.6763e+02mag3.2152e-03.bin; IC100K1.2213e+02mag6.8408e-03.bin; IC125K1.0315e+02mag1.4880e-03.bin; IC235K7.2640e+02mag3.6993e-02.bin; IC123K2.4714e+02mag7.2180e-03.bin; IC119K4.9624e+02mag3.1153e-02.bin; IC73K1.9292e+02mag4.1292e-02.bin; IC190K3.0921e+02mag7.6131e-02.bin; IC163K2.3874e+02mag2.6440e-02.bin; IC98K2.9143e+02mag5.0300e-02.bin; IC290K3.5223e+01mag6.1289e-03.bin; IC294K2.1680e+02mag2.5643e-03.bin; IC93K1.6320e+02mag9.3872e-02.bin; IC101K1.0784e+02mag5.1523e-02.bin; IC162K4.3853e+01mag1.8504e-01.bin; IC239K4.1655e+01mag2.4514e-03.bin; IC240K3.8638e+01mag1.9549e-02.bin; IC70K7.1608e+02mag4.1427e-01.bin

periods of libration and circulation. There is a small subset of integrations with approximately regular orbital behavior that do stably librate over long timescales.

### 3.1 High Amplitude, Chaotic Forcing

One representative example is presented in Figure 1, with variations in mean-motion attained from the corresponding REBOUND simulation presented in Figure 2. We can see a variety of behaviors in just this one simulation. First we notice that, due to the inherent chaos of the behavior of the orbital parameters from the input taken from the REBOUND simulation, the spin state also never reaches a true stable equilibrium. In this particular simulation, we see switching among different quasi-stable states, which each last on the order of a few thousand to tens of thousands of years. Some of these states include moderate-amplitude librations of  $\gamma$ , while others are states of complete circulation, wherein we observe full stellar coverage on the surface of the planet. We also note that, in the classical case of spin synchronization, there are two stable equilibria for  $\gamma$  at opposite longitudes: at 0 and at  $\pi$ , along the long axis of the planet. We do, in fact, observe state switches within the simulation depicted in Figure 1 where  $\gamma$  switches between librating about 0 and librating about  $\pi$ , as well as different circulating states where the spin direction in the co-rotating frame can change ( $\dot{\gamma} < 0$  versus  $\dot{\gamma} > 0$ ).

### 3.2 Stable Forcing

Other simulations can depict far more stable behavior if the behavior of the driving (i.e. the mean-motion) is also very stable. One such example is shown in Figure 3, where we show the evolution of  $\gamma$ ,  $\dot{\gamma}$ , and  $n$ , for a small period of time during the simulation (though the entire simulation depicts the same, stable behavior). We note the very regular behavior of the mean-motion  $n$ , especially as compared to the evolution of  $n$  for our other example shown Figure 2. In fact, the example depicted in Figure 3 is among the closest to our classical case presented in our previous paper (Vinson & Hansen 2017), where behavior of mean-motion  $n$  can largely be described as a simple pendulum with a single frequency. This can also be compared in Figures 4 and 5, which depict the Fourier Transforms of the mean-motion shown in Figure 2 and Figure 3, respectively. Where Figure 4 exhibits multiple frequencies in the mean-motion, in Figure 5 we see that the mean-motion is dominated by just one. As a result of a more stable mean-motion evolution, we observe a stable libration of  $\gamma$  in the 3 with an amplitude of about 0.4 radians about  $\pi$ .

### 3.3 Correlations

We can attempt to characterize the results of all of our 108 planetary history integrations in terms of the variance of  $\gamma$  and  $\dot{\gamma}$ . This can be difficult given the changing nature of individual simulations, but higher standard deviation of  $\dot{\gamma}$  about 0 (i.e. the *root mean squared*), and higher standard deviation of  $|\gamma|$  about its mean, would generally indicate cases of higher amplitude librations, or else even complete circulation that would result in effective stellar days. We denote our measures of the variance of  $\gamma$  and  $\dot{\gamma}$  as  $\sigma(\gamma)$  and  $\sigma(\dot{\gamma})$ , respectively.

With these variances, we can then attempt to relate the results to the REBOUND simulations which fed inputs to the spin model. We should then characterize the REBOUND simulations via terms that we would expect to have the strongest effects on the evolution of  $\gamma$ . In our previous work, we could largely describe the driving in

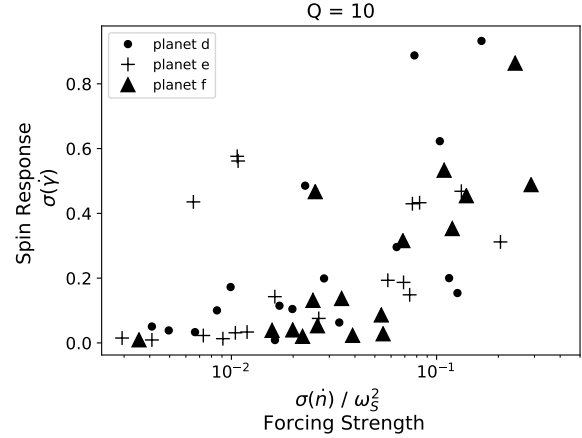


**Figure 6.** Standard deviation of  $\dot{\gamma}$  versus standard deviation of  $\dot{n}$  normalized to  $\omega_S^2$  for each of our integrations with tidal parameter  $Q = 10$  (i.e. higher tidal damping). Integrations for planets d, e, and f, are represented by dots, plus signs, and triangles, respectively. We see an overall trend that variations in  $\dot{\gamma}$  increase with variations in  $\dot{n}$ . Higher variations in  $\dot{\gamma}$  indicate larger responses to the driving of the spin argument  $\gamma$ , and thus would suggest the potential for larger total stellar coverage. Years are used for units with time.

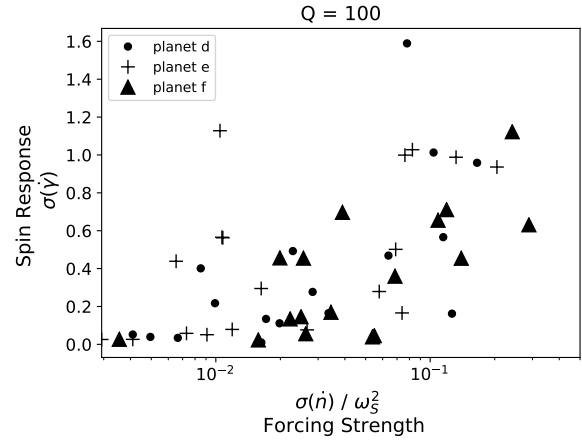


**Figure 7.** Standard deviation of  $\dot{\gamma}$  versus standard deviation of  $\dot{n}$  normalized to  $\omega_S^2$  for each of our integrations with tidal parameter  $Q = 100$  (i.e. lower tidal damping). Integrations for planets d, e, and f, are represented by dots, plus signs, and triangles, respectively. We see an overall trend that variations in  $\dot{\gamma}$  increase with variations in  $\dot{n}$ . Higher variations in  $\dot{\gamma}$  indicate larger responses to the driving of the spin argument  $\gamma$ , and thus would suggest the potential for larger total stellar coverage. Years are used for units with time.

terms of a driving frequency  $\omega_M$  (i.e. the frequency of variations of mean-motion  $n$ ), and in terms of an amplitude of the variations. In this work, the actual behavior of the driving is clearly more complex, but we can still attempt to largely characterize the simulations in terms of a frequency and of an amplitude of the driving. In reality, the chaotic behavior would result in varied amplitudes and multiple frequencies. But we can expect, and largely observe, a dominant frequency manifesting along with a typical amplitude.

We will therefore characterize the typical amplitude of the forcing as the standard deviation of  $\dot{n}$ , denoted  $\sigma(\dot{n})$ . We also take

a Fourier Transform to retrieve a primary frequency of oscillation from each of the REBOUND simulations, which we denote as  $\omega_M$ . As these values change depending on the REBOUND simulation, we can then relate these terms related to the driving to trends observed in the evolution of the spin argument  $\gamma$ . Finally, as we considered different forcing strengths and frequencies, we must also consider damping strengths. In this paper we consider two scenarios: strong damping with tidal  $Q = 10$ , and weak damping with  $Q = 100$ .

In figure 6 and 7, we demonstrate how variations in  $\dot{\gamma}$  respond to different levels of forcing by plotting  $\sigma(\dot{\gamma})$  versus a proxy for the amplitude of the forcing term in equation 3,  $\sigma(\dot{n})/\omega_S^2$ , for different tidal damping strengths,  $Q = 10$  and  $Q = 100$ , respectively. We normalize  $\sigma(\dot{n})$  to  $\omega_S^2$ , as this nondimensionalizes  $\sigma(\dot{n})$  to the torques on the spin and allows us to plot results from each of planets d, e, and f, on the same plot in a consistent manner, with  $\omega_S \approx 3.08 \text{ yr}^{-1}$ ,  $2.05 \text{ yr}^{-1}$ , and  $1.38 \text{ yr}^{-1}$  for planets d, e, and f, respectively, if eccentricity is small (valid for all these simulations). We note that these plots indeed show a correlation that as variations in  $\dot{n}$  grow, (i.e. the forcing strength in equation 3 increases), the spin responds more strongly with higher variations in  $\dot{\gamma}$ . There is also a clear dependence on tidal damping strengths, with higher tidal damping strength ( $Q = 10$ ) suppressing variations in  $\dot{\gamma}$  as compared to lower tidal damping strength ( $Q = 100$ ). We also note that each of these plots, while manifesting a correlation of  $\dot{\gamma}$  with  $\dot{n}$ , have a quite a bit of scatter. This is expected due to different dependencies with how the spin argument responds to the frequencies of variations in the mean-motion, which adds many complexities due to the chaotic nature of the mean-motion evolution in many of REBOUND integrations of the orbital parameters.

As we are largely interested in how the behavior of the spin affects the total stellar coverage of these planets, we also plot variations in the spin argument  $\gamma$ , which we denote with  $\sigma(\gamma)$ , versus  $\sigma(\dot{n})/\omega_S^2$  in Figures 8 and 9 for  $Q = 10$  and  $Q = 100$ , respectively. These figures then demonstrate how much the substellar point on these planets is varying in longitude over the course of our integrations. We expect  $\sigma(\gamma)$  to be about equal to zero for purely synchronous cases, and up to about  $\sigma(\gamma) = \pi/2$  for an ideal case where the spin exhibits full, regular, stellar days. In Figures 8 and 9 we can notice that many simulations have planets experiencing still spin-orbit synchronicity, with others experiencing some low to moderate-amplitude librations in  $\gamma$ , and some others experiencing very high amplitude librations or perhaps some periods of circulations, especially for those simulations experiencing higher variations in  $\dot{n}$ . We also note again that there are likely to be higher variations in  $\gamma$  for lower tidal damping strengths (i.e. *higher* tidal parameter  $Q$ ).

### 3.4 Timescales

There are two timescales which are of primary concern in our results for the spin evolution: one is the libration or circulation timescales, and the other is the duration of quasi-stable states, that we observe in many of our simulations. These timescales both would have profound implications for climate and thus for habitability.

The duration of quasi-stable states varies among our simulations from just a few thousand years to hundreds of thousands of years. In the example presented in Figure 1, we determine that the circulating and librating states endure on timescales on the order of  $10^4$  years. The planet would undergo long periods of moderate-amplitude librations of its spin argument  $\gamma$ , while occasionally switching to other quasi-stable states, some where spin argument  $\gamma$  can “flip” such that the side that was previously the “night side”

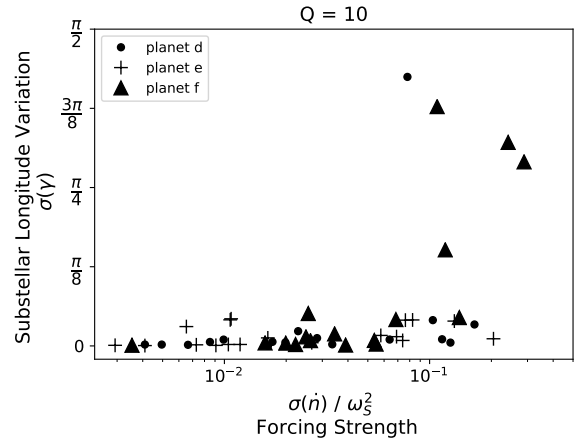


**Figure 8.** Standard deviation of  $\gamma$  versus standard deviation of  $\dot{n}$  normalized to  $\omega_S^2$  for each integration where set tidal parameter  $Q = 10$  (i.e. larger tidal damping). Planets d, e, and f, are represented with dots, plus signs, and triangles, respectively. We observe here that only a few planets experience very high variations in  $\gamma$  that would suggest large or complete stellar coverage. Years are used for units with time.

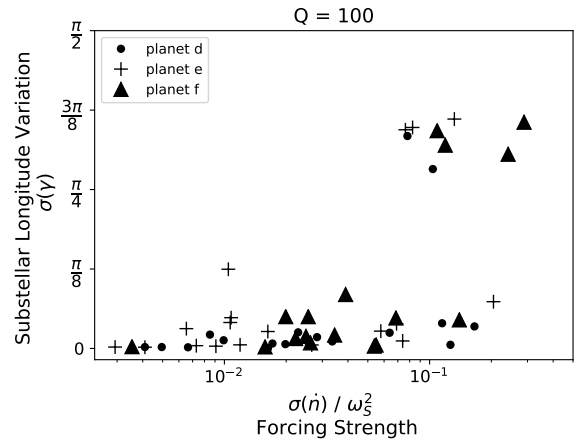


**Figure 9.** Standard deviation of  $\gamma$  versus standard deviation of  $\dot{n}$  normalized to  $\omega_S^2$  for each integration where set tidal parameter  $Q = 100$  (i.e. lower tidal damping). Planets d, e, and f, are represented with dots, plus signs, and triangles, respectively. We observe more planets here that experience very high variations in  $\gamma$  as compared to the highly damped cases ( $Q = 10$ ) showcased in Figure 8. Higher variations in  $\gamma$  suggest larger, or even complete, stellar coverage over time on the planet. We see clearly that there is higher probability of large variations in  $\gamma$  beyond a certain threshold in the standard deviation of  $\dot{n}$ . Years are used for units with time.

becomes the “day side” and vice versa, and other states where the spin argument  $\gamma$  can fully circulate for a few thousand years.

The other important timescale to note here is the period of the libration or circulation while in a quasi-stable state. Figure 10 and 11 depicts the average timescale for libration and circulation for each of our integrations for tidal parameters  $Q = 10$  and  $Q = 100$ , respectively. Here we see typical timescales on the order of a few years for both librating and circulating cases. This implies, for the circulating cases, full stellar days, wherein the planet makes a

full rotation in its co-rotating frame, which last on the order of a few years (while the system lasts in such a circulating quasi-stable state). We note that these stellar days last far longer than the orbital period of the planet, with the planet’s spin still being effectively synchronous over one orbit. We also note that circulating behavior is much more common for lower tidal damping strengths (corresponding to higher tidal parameter  $Q$ ), and also appears to be more common for the outer-most planet we simulated, planet f, and less common for inner-most simulated planet, planet d. This would also be expected, as the tidal damping strength, as well as depending on  $Q$ , also depends strongly on distance from the central star, with tidal damping increasing with decreased distance from the star. We note that circulation is still a possibility, however remote, even for planet d under the right circumstances.

#### 4 DISCUSSION

Our model depicts how much more complicated the spin states of planets in compact, multi-planet systems can be from what one might naively infer from simple tidal theory. The chaotic configuration of a system such as TRAPPIST-1 can lead to a chaotic driving of the spin argument  $\gamma$ , resulting in a variety of possible chaotic behaviors in the spin. Some simulations depict small or moderate amplitude librations of  $\gamma$ , while other depict full circulation, with many others exhibiting switches among different quasi-stable states. This can clearly have dramatic potential consequences on climate, and thus on habitability prospects.

From §3.4, we noted that the spin timescales for libration or circulation are on the order of a few years, as also seen in Figures 10 and 11. These timescales are shorter than the expected atmospheric response time of  $\lesssim 10$  years as calculated by Spiegel et al. (2008), and thus can help prevent atmospheric collapse on the night-side of the planet if the spin is circulating or undergoing high-amplitude libration.

We also note that state switching could also be likely, wherein the spin state changes behavior by abruptly transitioning from librating to circulating, circulating to librating, or else the planet swapping day and night sides for librating cases (e.g. switching from librating about  $\gamma$  at 0 to librating about  $\pi$  on the opposite face of the planet). The longevity of these quasi-stable states can last on the order of a few thousand years, though the time it takes to switch from one state to another is on the order of tens of years. This can result relatively stable climate states that last for a few thousand years, but that can then intermittently switch.

That the libration and circulation timescales are less than the expected atmospheric response times of these planets would seem to bode well for habitability prospects on these planets, if the response of the spin to the driving of mean-motion variations caused by neighboring planets is strong enough to produce high-amplitude librations in  $\gamma$ , or even complete circulation. The effects of the intermittent changes in climate, due to switches among quasi-stable spin states, is less certain. The time for the switches to occur would provide a period of transition on the order of tens of years from one quasi-stable climate period to another, likely giving the atmosphere enough time to respond gradually enough. More work is necessary to fully explore the effects on climate and the resultant effects on potential habitability.

With the new Transiting Exoplanet Survey Satellite (TESS), which aims to perform a near-full sky survey designed for detecting small exoplanets in tight configurations, there comes the opportunity of discovering many similar systems in which our model may be

applicable. We should note, however, that even given an optimistic scenario of getting many relevant analog systems from TESS, we wouldn’t expect to be able to observe any spin transitions occurring. Rather, we would observe a series of snapshots of the system.

#### 5 CONCLUSION

We have applied the spin model introduced in Vinson & Hansen (2017) more completely to different, stable configurations of the TRAPPIST-1 system. Studying different possible configurations and orbital histories of the system allowed us to more fully demonstrate possible spin behaviors for the system or systems like it. Our model showcases a range of possible responses of the spin behavior of a planet to the influences of nearby companions in resonant or near-resonant configurations.

We find that, for a system such as TRAPPIST-1, which contains seven planets in a long resonant chain, the resultant behavior of the spin can be varied and unpredictable. Such a multiple and compact system can have chaotic evolutions of orbital parameters, which could then cause chaotic evolutions of the spin. There can exist, however, quasi-stable spin states which remain stable for thousands of years before abruptly switching into a different quasi-stable state. Other simulations depict spin evolutions which are far less chaotic and are long-term stable (see Figure 3, which depicts a spin-state which is long-term stable and exhibits moderate-amplitude librations in the spin argument  $\gamma$ ).

These varied results suggest varied consequences for climate and habitability on these planets. It is often assumed that these planets orbiting so close to their host star must be tidally locked into synchronously rotating spin state, but our work here demonstrates that this isn’t necessarily the case. We show that, depending on factors such as the strength of variations in mean-motion due to the presence of nearby planetary companions, the spin of such planets may exhibit libration or even complete circulation, with timescales of libration and circulation on the order of years and shorter than the expected atmospheric response time. These results therefore should prompt further and more detailed investigation climate effects.

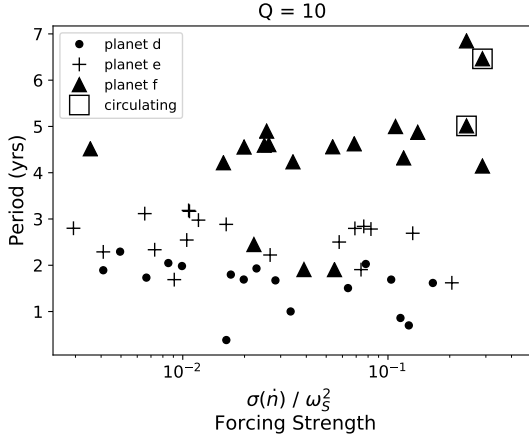


**Figure 10.** Periods of libration or circulation in  $\gamma$  plotted against variations in  $\dot{n}$  normalized to  $\omega_S^2$  for our integrations where we set tidal parameter  $Q = 10$  (i.e. higher tidal damping). Integrations for planets d, e, and f, are represented by dots, plus signs, and triangles, respectively. A square around one of these markers indicates a circulating timescale for the respective planet. We find that the timescales are all on the order of a few years, with only two of our integrations showcasing periods of time wherein the spin of the planet experiences circulating behavior.

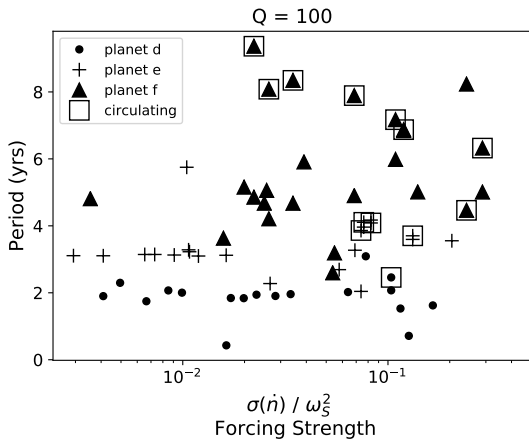


**Figure 11.** Periods of libration or circulation in  $\gamma$  plotted against variations in  $\dot{n}$  normalized to  $\omega_S^2$  for our integrations where we set tidal parameter  $Q = 100$  (i.e. lower tidal damping). Integrations for planets d, e, and f, are represented by dots, plus signs, and triangles, respectively. A square around one of these markers indicates a circulating timescale for the respective planet. We find that the timescales are all on the order of a few years, with more of these integrations showcasing periods of time wherein the spin of the planet experiences circulating behavior, as compared to the higher tidal damping cases showcased in Figure 10. We note that circulation in  $\gamma$  is most likely in planet f, and least likely in planet d.

## REFERENCES

Bolmont E., Selsis F., Owen J. E., Ribas I., Raymond S. N., Leconte J., Gillon M., 2017, *MNRAS*, **464**, 3728  
 Correia A. C. M., Boué G., Laskar J., Rodríguez A., 2014, *A&A*, **571**, A50  
 Efroimsky M., Lainey V., 2007, *Journal of Geophysical Research (Planets)*, **112**, E12003

Egbert G. D., Ray R. D., 2000, *Nature*, **405**, 775  
 Eggleton P. P., Kiseleva L. G., Hut P., 1998, *ApJ*, **499**, 853  
 Ferraz-Mello S., 2013, *Celestial Mechanics and Dynamical Astronomy*, **116**, 109  
 Gillon M. T., et al., 2017, *Nature Letters*, 542, 456  
 Goldreich P., Peale S., 1966, *AJ*, **71**, 425  
 Goldreich P., Peale S. J., 1968, *ARA&A*, **6**, 287  
 Grimm S. L., et al., 2018, *A&A*, **613**, A68  
 Hansen B. M. S., 2010, *ApJ*, **723**, 285  
 Hut P., 1981, *A&A*, **99**, 126  
 Joshi M., Haberle R., Reynolds R., 1997, *Icarus*, **129**, 450  
 Kasting J. F., Whitmire D. P., Reynolds R. T., 1993, *Icarus*, **101**, 108  
 Kopparapu R. K., et al., 2013, *ApJ*, **765**, 131  
 Kopparapu R. k., Wolf E. T., Haqq-Misra J., Yang J., Kasting J. F., Meadows V., Terrien R., Mahadevan S., 2016, *ApJ*, **819**, 84  
 Lainey V., Dehant V., Pätzold M., 2007, *A&A*, **465**, 1075  
 Makarov V. V., Efroimsky M., 2013, *ApJ*, **764**, 27  
 Millholland S., Wang S., Laughlin G., 2017, *The Astrophysical Journal Letters*, **849**, L33  
 Murray C. D., Dermott S. F., 1999, *Solar system dynamics*. Cambridge University Press, Cambridge  
 Ogilvie G. I., 2014, *ARA&A*, **52**, 171  
 Rein H., Liu S.-F., 2012, *Astronomy & Astrophysics*, **537**, A128  
 Rein H., Tamayo D., 2015, *Monthly Notices of the Royal Astronomical Society*, **452**, 376  
 Rein H., Tamayo D., 2017, *Monthly Notices of the Royal Astronomical Society*, **467**, 2377  
 Spiegel D. S., Menou K., Scharf C. A., 2008, *ApJ*, **681**, 1609  
 Tamayo D., Rein H., Petrovich C., Murray N., 2017, *ApJ*, **840**, L19  
 Vinson A. M., Hansen B. M. S., 2017, *MNRAS*, **472**, 3217  
 Weiss L. M., et al., 2018, *The Astronomical Journal*, **155**, 48  
 Wordsworth R., 2015, *The Astrophysical Journal*, **806**, 180